Cell Reports, Volume *37*

Supplemental information

Regulation of CYLD activity and specificity by phosphorylation and ubiquitin-binding CAP-Gly domains

Paul R. Elliott, Derek Leske, Jane Wagstaff, Lisa Schlicher, Georgina Berridge, Sarah Maslen, Frederik Timmermann, Biao Ma, Roman Fischer, Stefan M.V. Freund, David Komander, and Mads Gyrd-Hansen

Table S1. Data Collection and Refinement Statistics, Related to Figure 2.

	CYLD 464-552 + Ub	CYLD 464-565 + Ub
Data collection		
Beamline	Diamond I03	Diamond I03
Space group	$P\ 4_12_12$	$P\ 2_12_12_1$
a, *b*, *c* (Å)	43.93, 42.93, 171.34	63.93, 64.49, 75.93
α, β, γ (°)	90.00, 90.00, 90.00	90.00, 90.00, 90.00
Wavelength	0.96863	0.96863
Resolution (Å)	41.64-1.71 (1.74-1.71)	64.49-1.85 (1.89-1.85)
R_{merge}	4.2 (59.1)	6.1 (56.6)
$< I / \sigma I >$	15.0 (1.9)	14.0 (2.1)
CC(1/2)	0.99 (0.90)	0.99 (0.75)
Completeness (%)	100.0 (99.9)	100.0 (100.0)
Redundancy	6.0 (6.3)	6.3 (6.3)
Refinement		
Resolution (Å)	41.64 - 1.71	49.15 - 1.85
No. reflections (test set)	18,237	27,435
R_{work} / R_{free}	21.0/23.8	18.3/23.6
No. atoms		
Protein	1342	2658
Water	98	192
B-factors		
Wilson B	34.76	29.47
Protein	49.9	40.6
Water	55.1	46.4
R.m.s deviations		
Bond lengths (Å)	0.011	0.009
Bond angles (°)	1.174	1.017
Ramachandran statistics (outliers, allowed, favoured)	0.6, 3.8, 95.6	0.0, 1.5, 98.5

Numbers in brackets are for the highest resolution bin.
Datasets were collected and structures determined from a single crystal each.

Figure S1

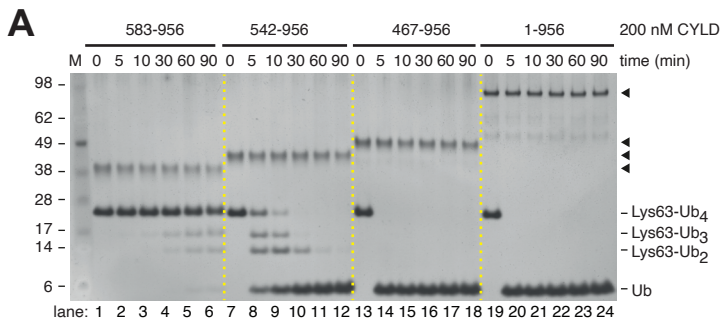
A
583-956
542-956
467-956
1-956
200 nM CYLD
M 0 5 10 30 60 90 0 5 10 30 60 90 0 5 10 30 60 90 0 5 10 30 60 90 time (min)
98
62
49
38
28
17
14
6
Lys63-Ub4
Lys63-Ub3
Lys63-Ub2
Ub
lane: 1 2 3 4 5 6 7 8 9 10 11 12 13 14 15 16 17 18 19 20 21 22 23 24

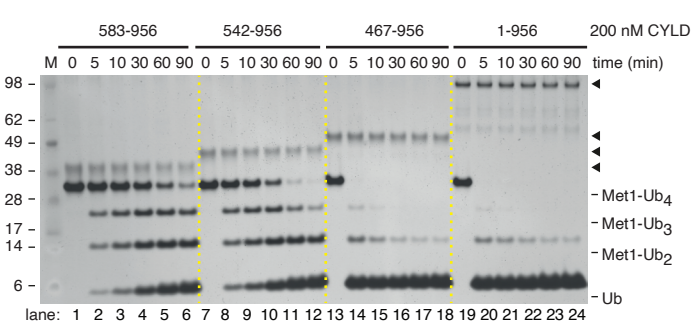
B
583-956
542-956
467-956
1-956
200 nM CYLD
M 0 5 10 30 60 90 0 5 10 30 60 90 0 5 10 30 60 90 0 5 10 30 60 90 time (min)
98
62
49
38
28
17
14
6
Met1-Ub4
Met1-Ub3
Met1-Ub2
Ub
lane: 1 2 3 4 5 6 7 8 9 10 11 12 13 14 15 16 17 18 19 20 21 22 23 24

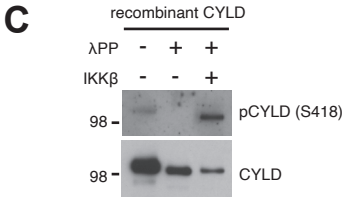
C
recombinant CYLD
λPP - + +
IKKβ - - +
98
pCYLD (S418)
98
CYLD

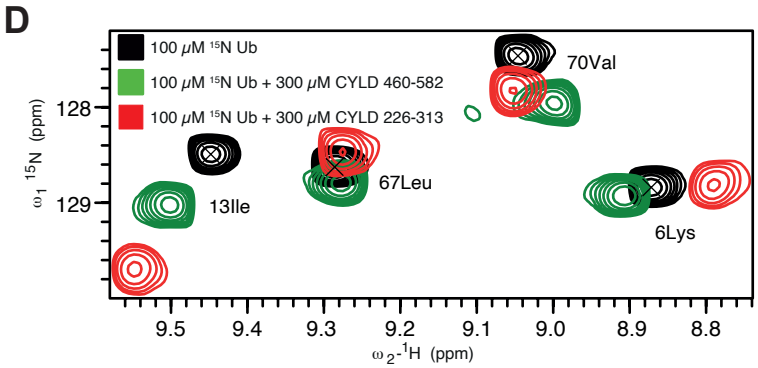
D
100 μM 15N Ub
100 μM 15N Ub + 300 μM CYLD 460-582
100 μM 15N Ub + 300 μM CYLD 226-313
70Val
67Leu
13Ile
6Lys
ω1 15N (ppm)
128
129
9.5 9.4 9.3 9.2 9.1 9.0 8.9 8.8
ω2-1H (ppm)

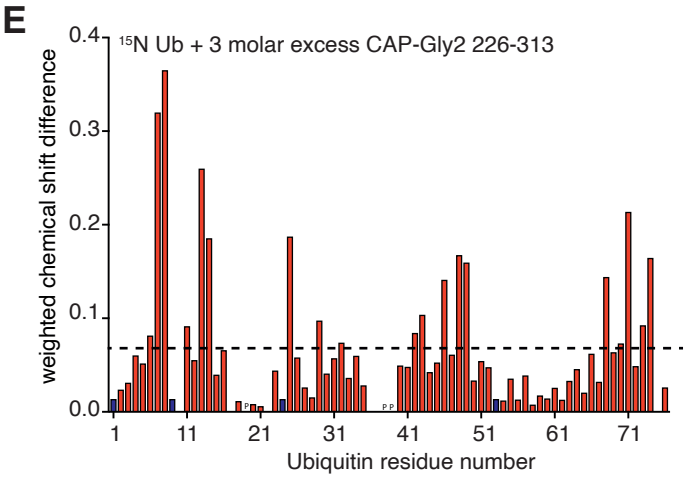
E
15N Ub + 3 molar excess CAP-Gly2 226-313
weighted chemical shift difference
0.4
0.3
0.2
0.1
0.0
1 11 21 31 41 51 61 71
Ubiquitin residue number

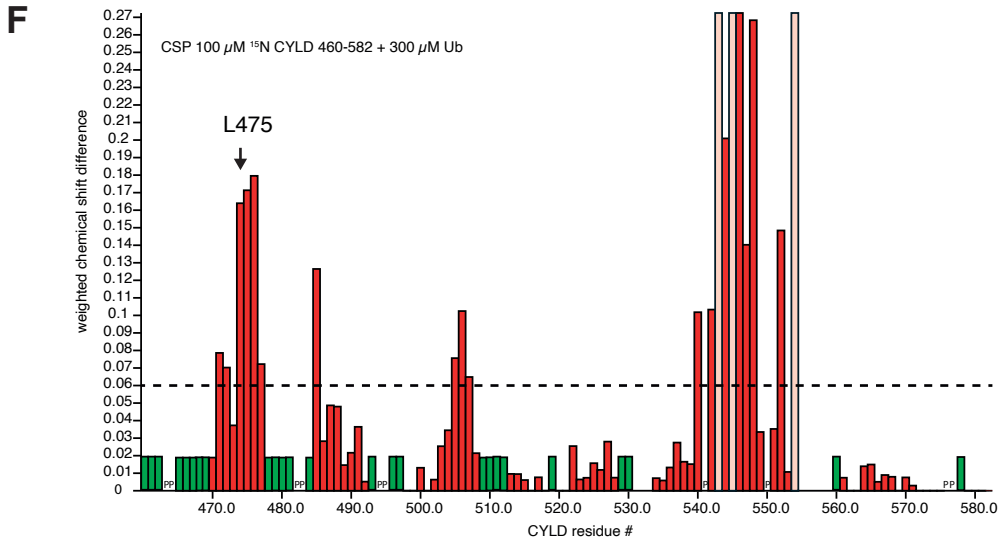
F
CSP 100 μM 15N CYLD 460-582 + 300 μM Ub
L475
weighted chemical shift difference
0.27
0.26
0.25
0.24
0.23
0.22
0.21
0.2
0.19
0.18
0.17
0.16
0.15
0.14
0.13
0.12
0.11
0.1
0.09
0.08
0.07
0.06
0.05
0.04
0.03
0.02
0.01
0
470.0 480.0 490.0 500.0 510.0 520.0 530.0 540.0 550.0 560.0 570.0 580.0
CYLD residue #

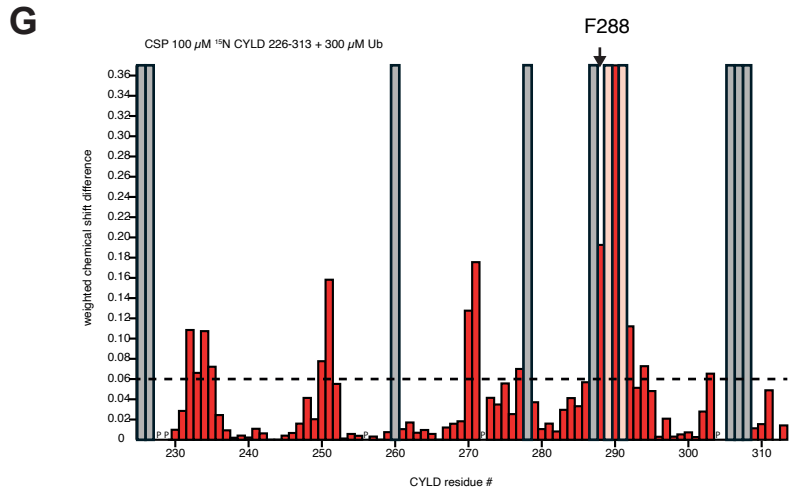
G
CSP 100 μM 15N CYLD 226-313 + 300 μM Ub
F288
weighted chemical shift difference
0.36
0.34
0.32
0.30
0.28
0.26
0.24
0.22
0.20
0.18
0.16
0.14
0.12
0.10
0.08
0.06
0.04
0.02
0
230 240 250 260 270 280 290 300 310
CYLD residue #

Figure S1: IKKβ phosphorylates CYLD *in vitro*, Related to Figure 1.

(A) Qualitative DUB assays for assessing CYLD enzyme activity. Lys63-Ub4 was incubated with different CYLD fragments (200 nM) and Ub cleavage was monitored over 90 minutes. Samples were resolved by SDS-PAGE and stained using silver stain. (B) Qualitative DUB assays as in (A) but using Met1 Ub4 as a substrate. (C) To investigate phosphorylation of CYLD by IKKβ, full-length CYLD purified from sf9 cells was treated with λPP. The λPP was subsequently removed by size exclusion chromatography and the dephosphorylated CYLD was either incubated with buffer alone (-) or IKKβ. Phosphorylation status of CYLD was determined by western blotting as indicated. (D) BEST-TROSY region for ^{15}N-labelled Ub (**Extended Data 1**) collected alone or in the presence of three-molar excess CAP-Gly2 (226-313) or CAP-Gly3 (460-582). (E) Chemical shift perturbation plot of ^{15}N-labelled Ub titrated with three-fold excess of CAP-Gly2 (226-313). (F) Chemical shift perturbation plot of ^{15}N-labelled CAP-Gly3 titrated with three-fold excess of Ub. (G) Chemical shift perturbation plot as in (F) with ^{15}N-labelled CAP-Gly2.

Figure S2

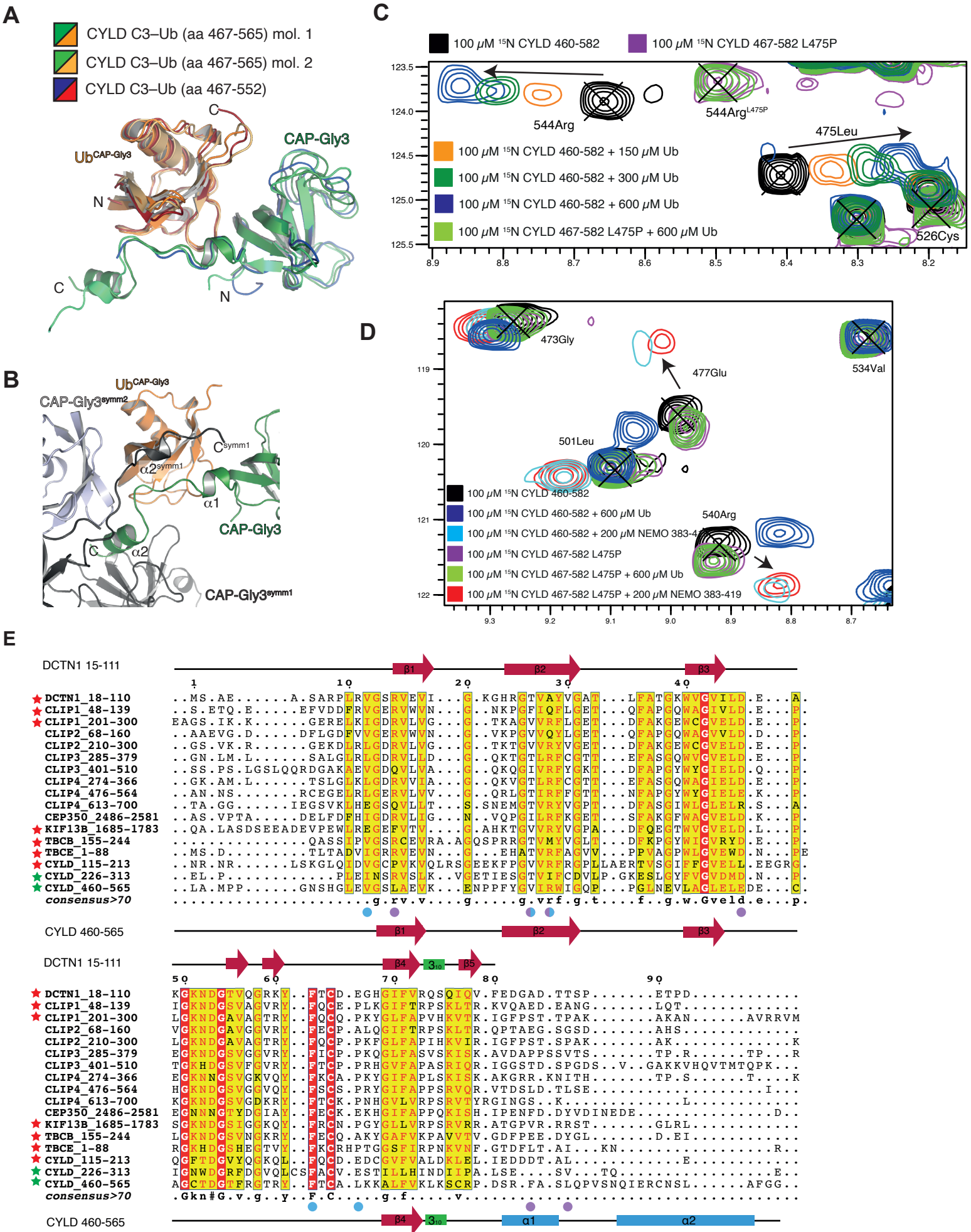
A
CYLD C3–Ub (aa 467-565) mol. 1
CYLD C3–Ub (aa 467-565) mol. 2
CYLD C3–Ub (aa 467-552)
Ub CAP-Gly3
CAP-Gly3
C
N
N
C
B
Ub CAP-Gly3
CAP-Gly3 symm2
C symm1
α2 symm1
α1
CAP-Gly3
C
α2
CAP-Gly3 symm1
C
100 μM 15N CYLD 460-582
100 μM 15N CYLD 467-582 L475P
544Arg
544Arg L475P
475Leu
100 μM 15N CYLD 460-582 + 150 μM Ub
100 μM 15N CYLD 460-582 + 300 μM Ub
100 μM 15N CYLD 460-582 + 600 μM Ub
100 μM 15N CYLD 467-582 L475P + 600 μM Ub
526Cys
123.5
124.0
124.5
125.0
125.5
8.9
8.8
8.7
8.6
8.5
8.4
8.3
8.2
D
473Gly
477Glu
534Val
501Leu
100 μM 15N CYLD 460-582
100 μM 15N CYLD 460-582 + 600 μM Ub
100 μM 15N CYLD 460-582 + 200 μM NEMO 383-419
100 μM 15N CYLD 467-582 L475P
100 μM 15N CYLD 467-582 L475P + 600 μM Ub
100 μM 15N CYLD 467-582 L475P + 200 μM NEMO 383-419
540Arg
119
120
121
122
9.3
9.2
9.1
9.0
8.9
8.8
8.7
E
DCTN1 15-111
β1
β2
β3
DCTN1_18-110
CLIP1_48-139
CLIP1_201-300
CLIP2_68-160
CLIP2_210-300
CLIP3_285-379
CLIP3_401-510
CLIP4_274-366
CLIP4_476-564
CLIP4_613-700
CEP350_2486-2581
KIF13B_1685-1783
TBCB_155-244
TBCE_1-88
CYLD_115-213
CYLD_226-313
CYLD_460-565
consensus>70
CYLD 460-565
β1
β2
β3
DCTN1 15-111
β4
3₁₀
β5
DCTN1_18-110
CLIP1_48-139
CLIP1_201-300
CLIP2_68-160
CLIP2_210-300
CLIP3_285-379
CLIP3_401-510
CLIP4_274-366
CLIP4_476-564
CLIP4_613-700
CEP350_2486-2581
KIF13B_1685-1783
TBCB_155-244
TBCE_1-88
CYLD_115-213
CYLD_226-313
CYLD_460-565
consensus>70
CYLD 460-565
β4
3₁₀
α1
α2
Ub contacts CAP-Gly2
Ub contacts CAP-Gly3

Figure S2: CAP-Gly domain 2 and 3 of CYLD bind Ub, Related to Figure 2.

(A) Superimposition of the two CAP-Gly3 molecules from crystal form 2 (467-565) (orthorhombic space group $P2_12_12_1$) and CAP-Gly3 (467-552) from crystal form 1 (tetragonal space group $P4_12_12$) onto one another, revealing low RMSD between the Ub orientation in all the structures obtained. (B) Crystal packing within crystal form 2 stabilizes helix α2 of CAP-Gly3 and positions Val551 against a separate interface of Ub. (C) BEST-TROSY region for ^{15}N-labelled CAP-Gly3 and the CAP-Gly3 Ub-binding mutant, L475P (**Extended Data 3-4**). The L475P mutation does not significantly alter the conformation of the CAP-Gly3 domain and is unable to bind Ub. (D) BEST-TROSY region for ^{15}N-labelled CAP-Gly3 and CAP-Gly3 L475P in the presence of six-fold molar excess of Ub or two-fold molar excess NEMO (383-419), revealing that mutation of the Ub binding interface does not affect NEMO binding. (E) Structure-based sequence alignment of all reported mammalian CAP-Gly domains. Secondary structure for DCTN1 CAP-Gly domain (18-110) is shown on top and CYLD CAP-Gly3 (460-565) is shown on the bottom. CAP-Gly2 and CAP-Gly3 residues that bind Ub are shown as blue and purple spheres respectively. CAP-Gly domains tested for Ub binding (**Extended Data 1**) that do not bind Ub are depicted as red stars, whereas CAP-Gly2 and CAP-Gly3 that bind Ub are represented as green stars.

Figure S3

A

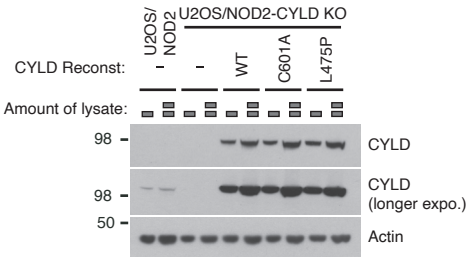
U2OS/
NOD2
U2OS/NOD2-CYLD KO
CYLD Reconst:
–
–
WT
C601A
L475P
Amount of lysate:
98
CYLD
98
CYLD
(longer expo.)
50
Actin

B

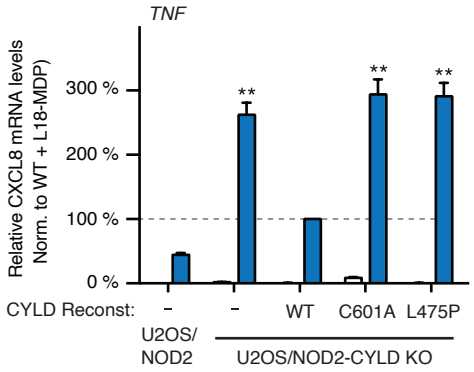
TNF
Relative CXCL8 mRNA levels
Norm. to WT + L18-MDP)
300 %
200 %
100 %
0 %
**
**
**
CYLD Reconst:
–
–
WT
C601A
L475P
U2OS/
NOD2
U2OS/NOD2-CYLD KO

Figure S3: CAP-Gly3 of CYLD is required for regulation of Ub deposition and signaling outcome, Related to Figure 3.

(A) Western blot analysis of CYLD levels in U2OS/NOD2 CYLD KO cells with reintroduced CYLD mutants as indicated. (B) qRT-PCR of U2OS/NOD2 CYLD KO cell lines with reintroduced CYLD mutants to assess *TNF* mRNA levels. Cells were stimulated for 3 h with 200 ng/ml L18-MDP. Values were normalized to values from L18-MDP-treated CYLD KO cells reconstituted with $CYLD^{WT}$. Data shown represents mean ±SEM of at least 3 independent experiments.

Figure S4

A

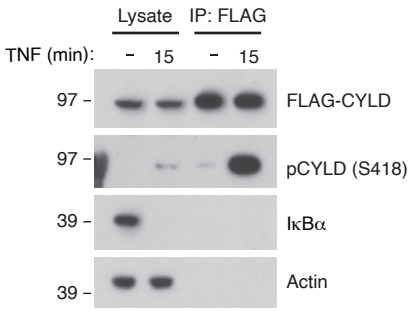
Lysate
IP: FLAG
TNF (min):
-
15
-
15
97 –
FLAG-CYLD
97 –
pCYLD (S418)
39 –
IκBα
39 –
Actin

Figure S4: TNF-induced phosphorylation of CYLD, Related to Figure 4.

(A) Immunoprecipitation of FLAG-tagged CYLD from lysates of U2OS/NOD2 CYLD KO cells expressing FLAG-CYLD^{WT} and stimulated or not with 20ng/ml TNF for 15 min. Lysates and IP samples were analyzed by western blotting as indicated before being processed for LC-MS/MS.

Figure S5

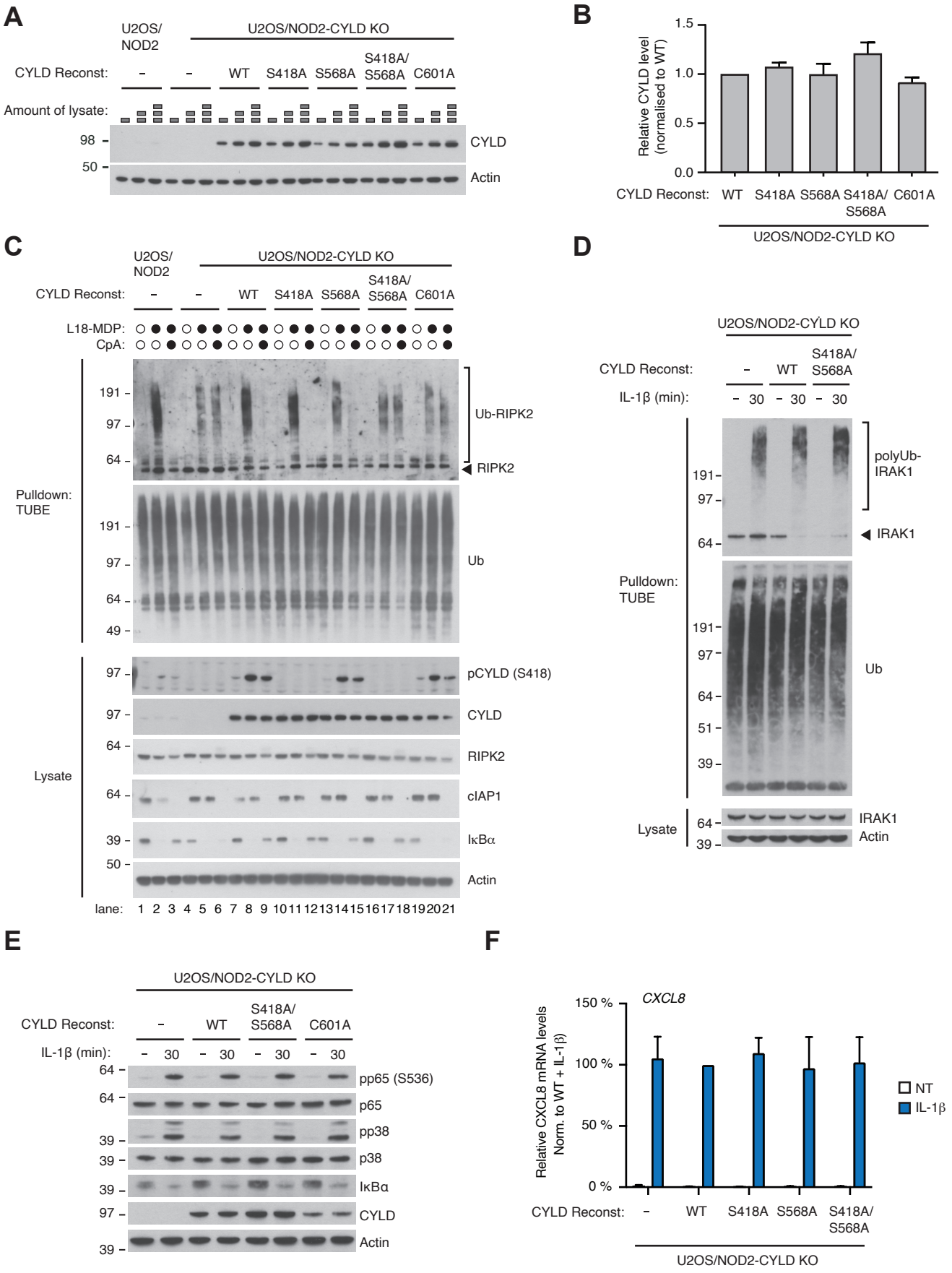
A
U2OS/ NOD2
U2OS/NOD2-CYLD KO
CYLD Reconst:
–
–
WT
S418A
S568A
S418A/ S568A
C601A
Amount of lysate:
98
50
CYLD
Actin
B
Relative CYLD level (normalised to WT)
1.5
1.0
0.5
0.0
CYLD Reconst:
WT
S418A
S568A
S418A/ S568A
C601A
U2OS/NOD2-CYLD KO
C
U2OS/ NOD2
U2OS/NOD2-CYLD KO
CYLD Reconst:
L18-MDP:
CpA:
Pulldown: TUBE
191
97
64
49
Ub-RIPK2
RIPK2
Ub
Lysate
97
64
39
50
pCYLD (S418)
CYLD
RIPK2
cIAP1
IκBα
Actin
lane: 1 2 3 4 5 6 7 8 9 10 11 12 13 14 15 16 17 18 19 20 21
D
U2OS/NOD2-CYLD KO
CYLD Reconst:
–
WT
S418A/ S568A
IL-1β (min):
– 30 – 30 – 30
Pulldown: TUBE
191
97
64
51
39
polyUb-IRAK1
IRAK1
Ub
Lysate
IRAK1
Actin
E
U2OS/NOD2-CYLD KO
CYLD Reconst:
–
WT
S418A/ S568A
C601A
IL-1β (min):
– 30 – 30 – 30 – 30
64
39
97
pp65 (S536)
p65
pp38
p38
IκBα
CYLD
Actin
F
CXCL8
Relative CXCL8 mRNA levels Norm. to WT + IL-1β)
150 %
100 %
50 %
0 %
NT
IL-1β
CYLD Reconst:
–
WT
S418A
S568A
S418A/ S568A
U2OS/NOD2-CYLD KO

Figure S5: Ser568 phosphorylation together with Ser418 regulates CYLDs ability to control Ub deposition and signaling outcome after NOD2 but not IL-1β receptor stimulation, Related to Figure 5.

(A) Western blot analysis of CYLD levels in U2OS/NOD2 CYLD KO cells reconstituted with CYLD variants as indicated. (B) Densitometric quantification of CYLD levels in (A). Data shown represents mean ±SEM of 2 values. (C) Purification and western blot analysis of Ub conjugates from U2OS/NOD2 cell lines. Cells were treated for 1 h with CpA (1 μM) or DMSO prior to stimulation with 200 ng/ml L18-MDP for 1 h as indicated. Repeat experiment of data shown in Figure 5C to illustrate the partial reversal of RIPK2-Ub in cells expressing CYLD S568A. (D) Purification and western blot analysis of Ub conjugates from U2OS/NOD2 cell lines. Cells were treated for 30 min with 20 ng/ml IL-1β as indicated. (E) Western blot analysis to assess signaling after IL-1β treatment. Cells were treated with 10 ng/ml IL-1β for 30 min as indicated. (F) Relative levels of *CXCL8* mRNA in U2OS/NOD2 cell lines treated or not with 10 ng/ml IL-1β for 3 h. Data shown represents mean ±SEM of at least 3 independent experiments. *$p < 0.05$, **$p < 0.01$, *n.s.,* not significant.

Figure S6

A

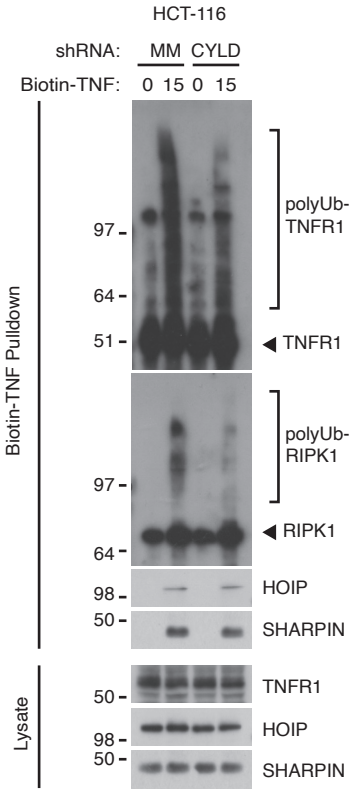
HCT-116
shRNA: MM CYLD
Biotin-TNF: 0 15 0 15
Biotin-TNF Pulldown
97
64
51
polyUb-TNFR1
TNFR1
97
64
polyUb-RIPK1
RIPK1
98
50
HOIP
SHARPIN
Lysate
50
98
50
TNFR1
HOIP
SHARPIN

Figure S6: The absence of CYLD activity interferes with ubiquitination of TNF-RSC components, Related to Figure 6.

(A) Purification and western blot analysis of the TNFR1 complex in HCT-116 cells with shRNA knockdown of CYLD or mismatch control. Cells were stimulated with 50 ng/ml Biotin-TNF for indicated time points. Samples used for western blots analysis are from the same experiment shown in Figure 4B.

Figure S7

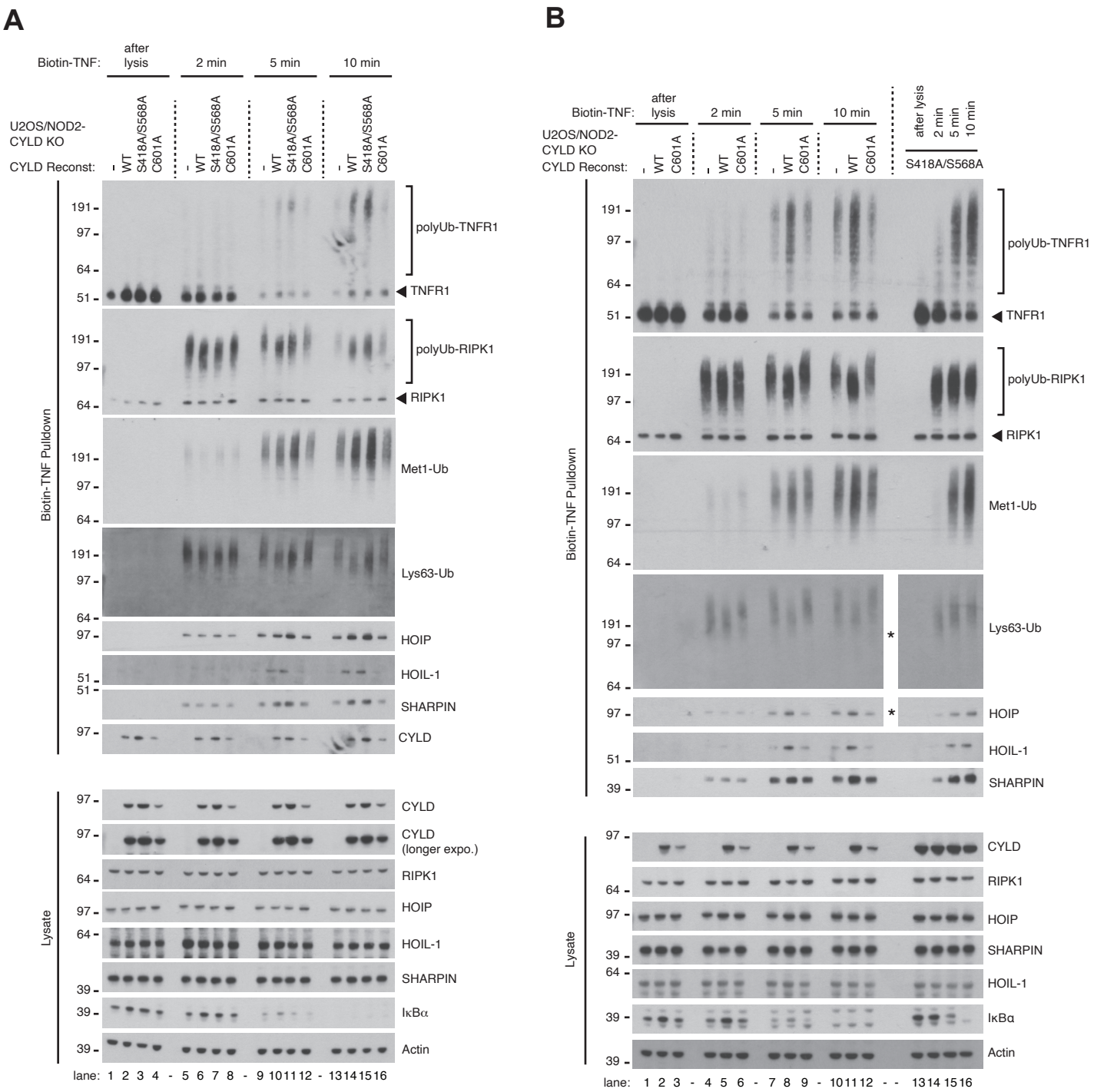
A
Biotin-TNF:
after lysis
2 min
5 min
10 min
U2OS/NOD2-CYLD KO
CYLD Reconst:
-
WT
S418A/S568A
C601A
Biotin-TNF Pulldown
polyUb-TNFR1
TNFR1
polyUb-RIPK1
RIPK1
Met1-Ub
Lys63-Ub
HOIP
HOIL-1
SHARPIN
CYLD
Lysate
CYLD
CYLD (longer expo.)
RIPK1
HOIP
HOIL-1
SHARPIN
IκBα
Actin
lane: 1 2 3 4 - 5 6 7 8 - 9 10 11 12 - 13 14 15 16
B
Biotin-TNF:
after lysis
2 min
5 min
10 min
after lysis
2 min
5 min
10 min
U2OS/NOD2-CYLD KO
CYLD Reconst:
-
WT
C601A
S418A/S568A
Biotin-TNF Pulldown
polyUb-TNFR1
TNFR1
polyUb-RIPK1
RIPK1
Met1-Ub
Lys63-Ub
HOIP
HOIL-1
SHARPIN
Lysate
CYLD
RIPK1
HOIP
SHARPIN
HOIL-1
IκBα
Actin
lane: 1 2 3 - 4 5 6 - 7 8 9 - 10 11 12 - - 13 14 15 16

Figure S7: Non-phosphorylation-mediated activity of CYLD retains LUBAC at the TNF-RSC and restores normal Met1-Ub, but not Lys63-Ub, deposition, Related to Figure 7.

(A and B) Independent repeats of the data shown in Figure 7A. Purification and western blot analysis of the TNFR1 complex in U2OS/NOD2 cell lines as indicated. Cells were stimulated with 50 ng/ml Biotin-TNF for indicated time points. Lanes 1-12 in (B) are also shown in Figure 6C. Asterisks in (B) indicate that the scanned blots for Lys63-Ub and HOIP have been cut and reassembled to align with other blots in the figure. Due to a loading error the CYLD$^{S418A/S586A}$ samples (lanes 13-16) were shifted one lane relative to the other blots.

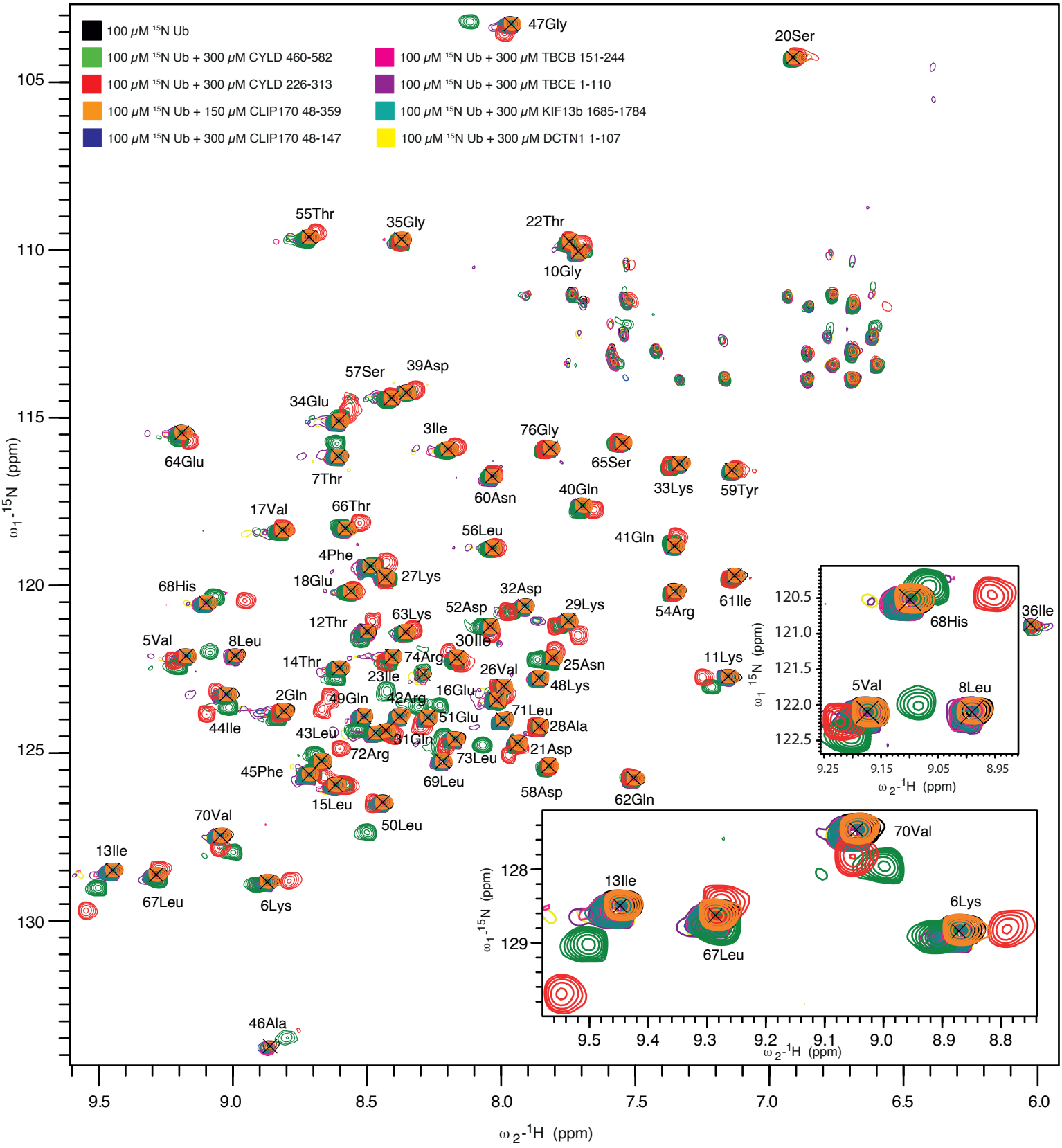
100 μM ¹⁵N Ub
100 μM ¹⁵N Ub + 300 μM CYLD 460-582
100 μM ¹⁵N Ub + 300 μM CYLD 226-313
100 μM ¹⁵N Ub + 150 μM CLIP170 48-359
100 μM ¹⁵N Ub + 300 μM CLIP170 48-147
100 μM ¹⁵N Ub + 300 μM TBCB 151-244
100 μM ¹⁵N Ub + 300 μM TBCE 1-110
100 μM ¹⁵N Ub + 300 μM KIF13b 1685-1784
100 μM ¹⁵N Ub + 300 μM DCTN1 1-107
ω1-15N (ppm)
ω2-1H (ppm)
47Gly
20Ser
55Thr
35Gly
22Thr
10Gly
57Ser
39Asp
34Glu
3Ile
76Gly
64Glu
7Thr
65Ser
33Lys
59Tyr
60Asn
40Gln
17Val
66Thr
56Leu
41Gln
4Phe
68His
18Glu
27Lys
32Asp
54Arg
61Ile
52Asp
29Lys
12Thr
63Lys
30Ile
5Val
8Leu
14Thr
74Arg
25Asn
23Ile
26Val
11Lys
48Lys
2Gln
16Glu
49Gln
42Arg
71Leu
44Ile
51Glu
28Ala
43Leu
31Gln
72Arg
73Leu
21Asp
45Phe
69Leu
58Asp
62Gln
15Leu
50Leu
70Val
13Ile
67Leu
6Lys
46Ala
36Ile

Extended Data 1. Map of chemical shift perturbations, Related to Figure 1.

BEST-TROSY spectra for ^{15}N-labelled Ub alone (black) or in the presence of three-fold molar excess CAP-Gly domains. Chemical shift perturbations are only observed for CYLD CAP-Gly2 and CAP-Gly3 domains, green and red respectively. Residue numbers correspond to resonance assignment of Ub are shown.

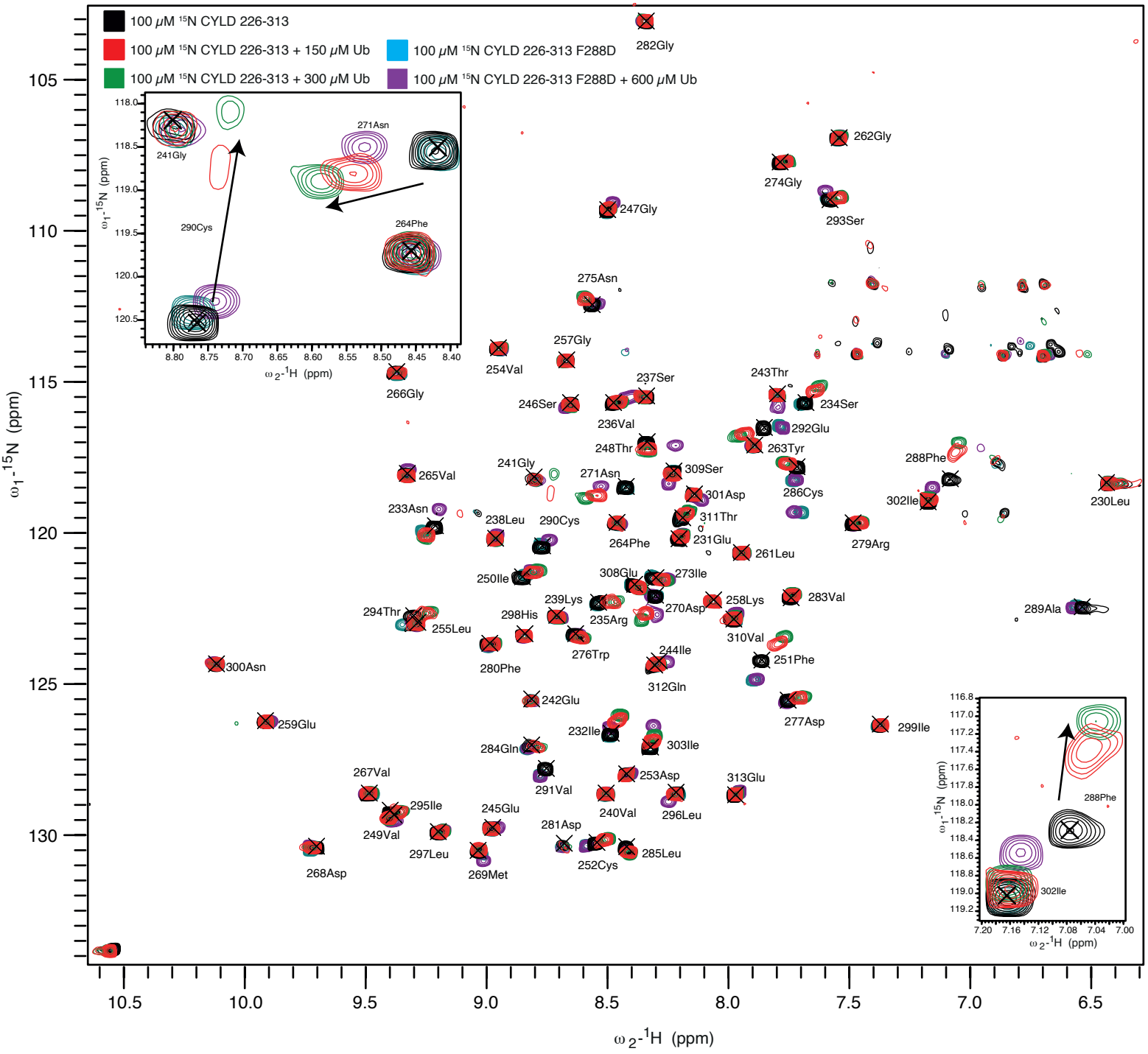
100 μM ¹⁵N CYLD 226-313
100 μM ¹⁵N CYLD 226-313 + 150 μM Ub
100 μM ¹⁵N CYLD 226-313 F288D
100 μM ¹⁵N CYLD 226-313 + 300 μM Ub
100 μM ¹⁵N CYLD 226-313 F288D + 600 μM Ub
ω1-15N (ppm)
ω2-1H (ppm)
241Gly
271Asn
290Cys
264Phe
288Phe
302Ile
282Gly
262Gly
274Gly
293Ser
247Gly
275Asn
257Gly
254Val
266Gly
237Ser
246Ser
236Val
243Thr
234Ser
292Glu
263Tyr
248Thr
309Ser
265Val
241Gly
271Asn
301Asp
286Cys
233Asn
238Leu
290Cys
311Thr
264Phe
231Glu
279Arg
230Leu
261Leu
250Ile
308Glu
273Ile
239Lys
270Asp
258Lys
283Val
289Ala
294Thr
255Leu
298His
235Arg
310Val
280Phe
276Trp
244Ile
251Phe
300Asn
312Gln
242Glu
277Asp
299Ile
259Glu
232Ile
303Ile
284Gln
313Glu
267Val
291Val
253Asp
295Ile
240Val
296Leu
249Val
245Glu
281Asp
297Leu
285Leu
268Asp
269Met
252Cys

Extended Data 2. Map of chemical shift perturbations, Related to Figure 2.

BEST-TROSY spectra for ^{15}N-labelled CAP-Gly2 (black) or CAP-Gly2 F288D (blue) alone or in the presence of increasing concentrations of Ub. Complete backbone assignment of ^{13}C, ^{15}N CAP-Gly2 resonances permitted detailed interactions between CAP-Gly2 and Ub to be observed. Insert two regions show detailed titration of resonances Cys290 and Phe288.

Extended data 3

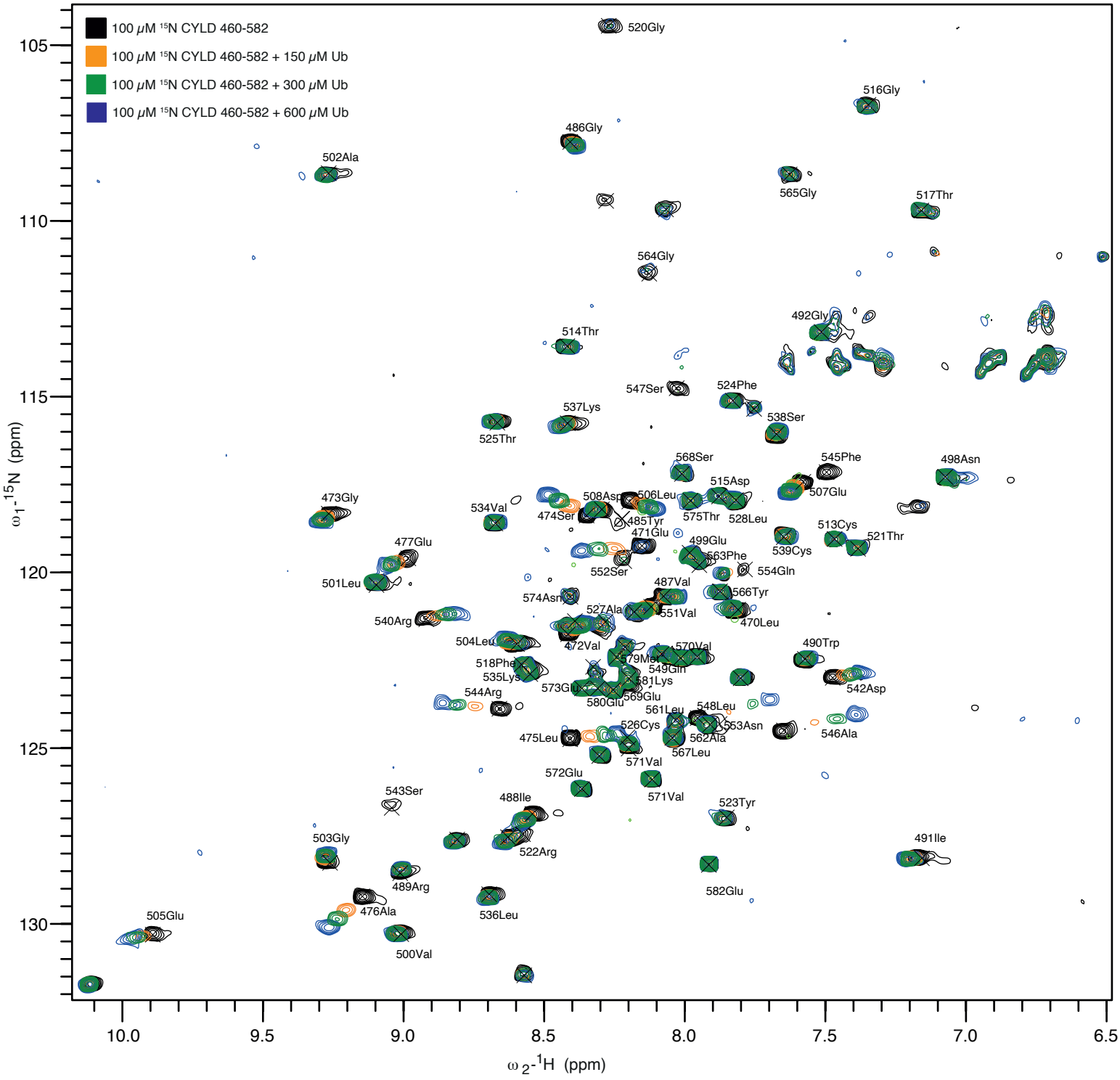

Extended Data 3. Map of chemical shift perturbations, Related to Figure 2.

BEST-TROSY spectra for ^{15}N-labelled CAP-Gly3 (black) with increasing concentrations of Ub. Resonance positions for CAP-Gly3 amino acids derived from complete backbone assignment of ^{13}C, ^{15}N CAP-Gly3 (460-582) spectra are shown.

Extended data 4

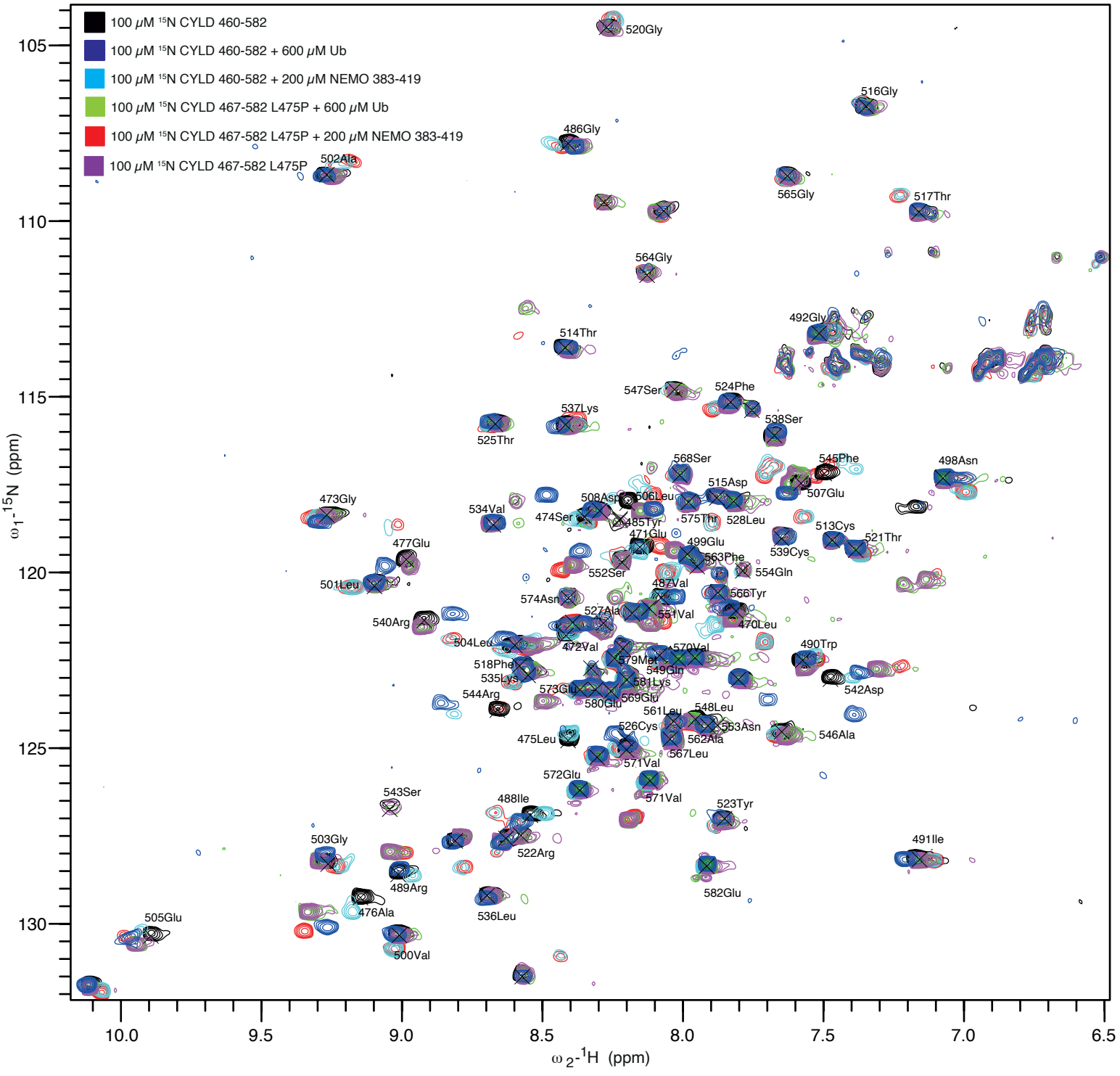

Extended Data 4. Map of chemical shift perturbations, Related to Figure 2.

BEST-TROSY spectra for ^{15}N-labelled CAP-Gly3 (black) in the presence of six-fold molar excess of Ub (dark blue) or two-fold molar excess of NEMO (light blue). The CAP-Gly3 Ub-binding mutant L475P, was recorded alone (purple) or in the presence of six-fold molar excess NEMO (red) exhibited similar chemical shift perturbations as WT CAP-Gly3. However, L475P is does not undergo any chemical shift perturbations in the presence of six-fold molar excess Ub (green).